Acousto-Optic Diffraction by Shear Horizontal Surface Acoustic Waves in 36° Rotated *Y*-Cut *X*-Propagation Lithium Tantalate

R. Rimeika[a], D. Čiplys[a] and M. Shur[b]
[a]Department of Radiophysics, Vilnius University, Vilnius, Lithuania
[b]ECSE, and PAPA, Rensselaer Polytechnic Institute, Troy, NY, USA

We have investigated the acousto-optic diffraction by shear horizontal surface acoustic waves in 36° rotated *Y*-cut *X*-propagation lithium tantalate ($LiTaO_3$) crystals. The measurements were performed at the optical wavelength 633 nm of He–Ne laser and acoustic wavelengths of 50–60 μm. The anisotropic diffraction with the light polarization rotation in the transmission mode was observed. The measured and calculated values of the light incidence angle corresponding to the strongest diffraction differed significantly. A narrow strip of a thin metal film deposited on the crystal surface drastically affected the light diffraction. We attribute these effects to the conversion processes between the shear horizontal leaky surface acoustic wave and shear horizontal surface skimming bulk wave.

DOI: 10.12693/APhysPolA.127.52
PACS: 77.65.Dq, 43.35.Sx, 78.20.hb

1. Introduction

Shear horizontal surface acoustic waves (SH SAWs) in piezoelectric crystals are very attractive for applications in telecommunications, signal processing, and sensing technologies. The 36° rotated *Y*-cut *X*-propagation $LiTaO_3$ single crystals are amongst the most usable substrates supporting the SH SAWs, due to the very low propagation loss on this specific cut [1, 2]. The advantages of SH SAWs in comparison with the conventional Rayleigh waves are: a higher propagation velocity, allowing for a higher frequency operation; capability to propagate on the solid-liquid interface, making the SH SAWs very suitable for liquid-media sensors. The radio-frequency (RF) filters for telecommunication applications and various physical and chemical sensors on the basis of the 36° rotated *YX* $LiTaO_3$ have been reported [3, 4]. Therefore, the studies of SH SAW propagation and interaction are of great interest. The acousto-optic technique presents an efficient tool for such studies. However, the acousto-optic investigations in 36° rotated *YX* $LiTaO_3$ are very scarce [5, 6]. The goal of the present work was to fill in this gap. We report on the dramatic effect on the light diffraction from the SH SAWs in 36° rotated *YX* $LiTaO_3$ caused by a thin-film metal strip deposited on the crystal surface.

2. Experimental technique

The interdigital transducers (IDTs) with periodicity of 50 μm or 60 μm were deposited by standard photolithography. The fabricated samples were characterized by measuring the SAW transmission vs. frequency characteristics using a radio-frequency network analyzer.

Figure 1 shows the experimental setup for acousto-optic measurements. The sample under investigation was mounted on the translation stage on top of the rotary table of the single-axis optical goniometer. The tuneable radio-frequency (RF) pulse oscillator was used for the SAW excitation. The pulse width was about 1 μs, and the RF power was up to 1 W into the matched load of 50 Ω. The He–Ne laser light with the wavelength of 633 nm was incident on the SAW propagation path, and the light diffracted by the SAW was detected by the photomultiplier tube (PMT) mounted on the rotating arm of the goniometer. The SH SAWs very weakly affected the reflected light because no significant surface curvature was created. The transmitted light was diffracted by the SH SAW due to the elasto-optic modulation of the refractive index in the sub-surface region of the acoustic wave confinement. The optical polarizer was used to analyze the diffracted beam. The PMT and RF oscillator output signals were observed with the oscilloscope. The measurements of the diffracted light intensity and light incidence angle were performed at the different positions of the diffraction point along the SAW propagation direction. The diffraction was measured on the free sample surface and on the surface with a narrow strip of thin

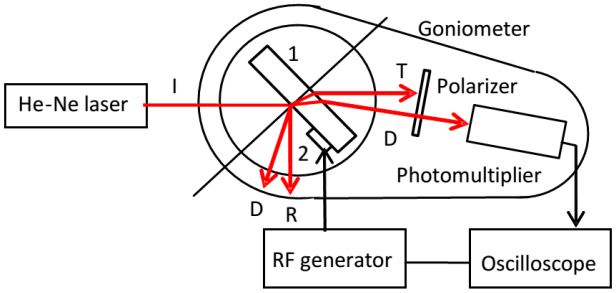

Fig. 1. Experimental setup. 1 — $LiTaO_3$ substrate, 2 — interdigital transducer; light beams: I — incident, R — reflected, T — transmitted, D — diffracted.

copper film deposited on the SAW path by thermal evaporation. The width of the strip was 1 mm, and the spacing between the strip and transmitting IDT was 3.6 mm.

3. Results and discussion

3.1. SAW transmission

Figure 2 shows the transmission characteristic measured with the RF network analyzer in a wide frequency range for the sample with the 50 μm IDTs. The transmission maxima corresponding to the two types of SAWs were observed: Rayleigh wave at 63 MHz and SH SAW at 83.2 MHz. They correspond to the velocities 3.15 km/s and 4.16 km/s, respectively, determined as $V = \Lambda f$, where Λ is the IDT period, and f is the frequency of SAW excitation peak. These velocity values are in good agreement with those reported in literature [2]. The significantly stronger transmission of the SH wave implies its much higher excitation efficiency, in agreement with the theoretical values of electromechanical coupling coefficient 0.046% for Rayleigh waves and 4.7% for SH SAW [2]. Similar results were obtained for the sample with the 60 μm IDTs, exhibiting the Rayleigh and SH SAW maxima at 52.5 MHz and 68 MHz, respectively.

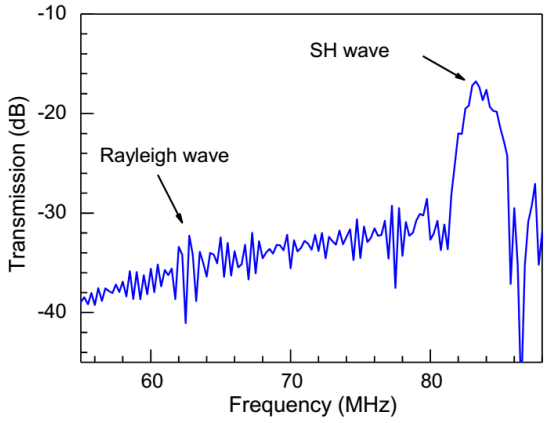

Fig. 2. SAW transmission in 36° rotated YX $LiTaO_3$ measured with the network analyzer for a sample with 50 μm period transducers.

3.2. Light incidence angle

Our observations showed that the diffraction in transmission mode took place at a specific value of light incidence angle with the polarization of the diffracted light being normal to that of the incident light. This implies the anisotropic diffraction, in contrast to the isotropic diffraction by the Rayleigh wave observed in the reflection mode at any light incidence angle and with no change in the light polarization.

The light incidence angle for the anisotropic diffraction must satisfy the phase matching condition, which is depicted in Fig. 3 for the extraordinary light beam incident at the angle Θ_i. From the configuration of the interacting wave vectors, one obtains

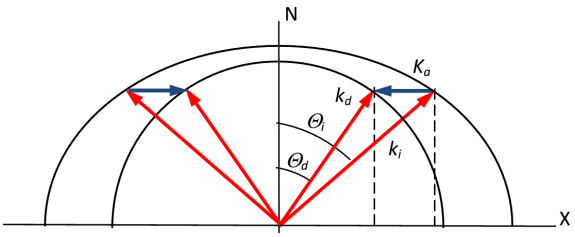

Fig. 3. Configuration of interacting wave vectors: $\boldsymbol{k}_\mathrm{i}$, incident light; $\boldsymbol{K}_\mathrm{a}$, acoustic wave; $\boldsymbol{k}_\mathrm{d}$, diffracted light; N is the surface normal, and X is the crystallographic axis.

$$n\left(\Theta_\mathrm{i}\right)\sin\Theta_\mathrm{i} - \left[n_\mathrm{o}^2 - \left(n\left(\Theta_\mathrm{i}\right)\cos\Theta_\mathrm{i}\right)^2\right]^{1/2} = \frac{\lambda_0}{\Lambda}, \qquad (1)$$

where λ_0 and Λ are the optical wavelength in a free space and the acoustic wavelength, respectively; the direction-dependent refractive index for the incident wave is

$$n\left(\Theta_\mathrm{i}\right) = \frac{n_\mathrm{e}}{\sqrt{1+\cos^2\Theta_\mathrm{i}\sin^2 36^\circ\left[\left(n_\mathrm{e}/n_\mathrm{o}\right)^2-1\right]}}, \qquad (2)$$

and n_o and n_e are the ordinary and extraordinary refractive indices of the crystal, respectively. The diffracted light corresponds to the ordinary beam and propagates at the angle Θ_d, which is determined from the relation

$$\cos\Theta_\mathrm{d} = \frac{n\left(\Theta_\mathrm{i}\right)}{n_\mathrm{o}}\cos\Theta_\mathrm{i}. \qquad (3)$$

Substituting the values of refractive indices $n_\mathrm{o} = 2.176$ and $n_\mathrm{e} = 2.18$ [7] for optical wavelength of 633 nm yields the incidence angles for acousto-optic diffraction with conversion from extraordinary to ordinary beam of 15.7 deg and 19.3 deg at the acoustic wavelengths of 50 μm and 60 μm, respectively. These are "internal" incidence angles in the crystal. The "external" angles of light incidence onto the sample surface (36.2 deg and 45.9 deg at 50 μm and 60 μm SH SAW wavelengths, respectively) are calculated from Snell's law for the light refraction at the air–crystal interface.

Figure 4 shows the dependences of the diffracted light intensity on the light incidence angle measured at SH SAW frequency of 68 MHz corresponding to the 60 μm wavelength. The measurements on a free sample surface were performed at different distances from the exciting IDT along the SAW propagation direction. Curves 1 and 2 in Fig. 4 represent two positions of the diffraction point. The striking evidence is that the diffraction peaks at different light spot positions were observed at different angles of the light incidence, and the measured angle values were much lower than those calculated above from the phase-matching condition (1).

The dependence of the light incidence angle as a function of diffraction point position is plotted in Fig. 5. Curve 1 corresponds to the free sample surface. As the light spot moved away from the IDT, the incidence angle corresponding to the diffraction maximum increased, but did not reach the calculated value over the distance of 13 mm. Our observations cannot be explained on the basis of configuration depicted in Fig. 3.

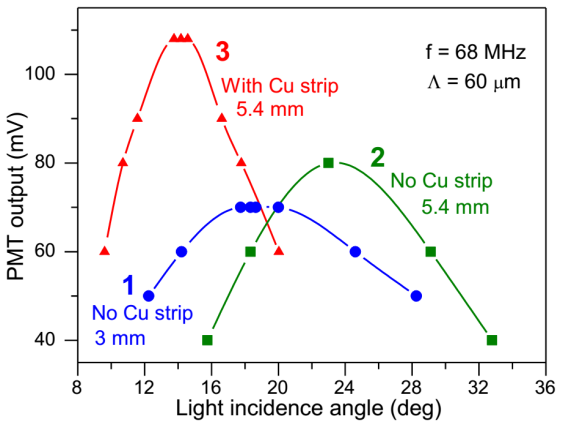

Fig. 4. Dependences of diffracted light intensity on light incidence angle measured at different distances of light spot from IDT (indicated at the curves) on the crystal surface without (1, 2) and with Cu-film strip (3).

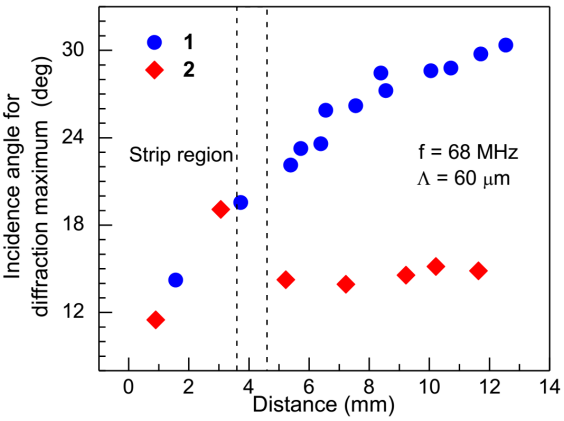

Fig. 5. Light incidence angle corresponding to maximum light diffraction as a function of light spot distance from IDT on the crystal surface without (1) and with (2) Cu-film strip.

A more sophisticated model, beyond the scope of the present work, should account for possible variations in the acoustic wave vector direction.

3.3. Effect of metal–film strip

Our experiments revealed that the diffracted light signal was strongly affected by a thin copper (Cu) film strip deposited on the $LiTaO_3$ plate surface at some distance from the diffraction point. Curve 3 of Fig. 4 represents the dependence of diffracted light intensity on the light incidence angle for the diffraction point located on the free sample surface behind the Cu film strip. Curve 2 of Fig. 4 was measured at the same point of the sample surface in the absence of the Cu strip. As seen, the presence of the strip dramatically reduces the light incidence angle and increases the diffraction efficiency. Curve 2 of Fig. 5 shows the dependence of the light incidence angle (corresponding to the diffraction maximum) versus the light spot position measured in the presence of the Cu strip. In the region, where the SAW travels from the IDT to the strip, the latter introduces no changes. Clearly, the diffraction measurements could not be performed in the strip region, which blocked the light transmission. After the SAW passes the strip, the maximum-diffraction light incidence angle remained practically constant. Its value was much less than that measured on the sample surface without the strip (curve 1 of Fig. 5). Figures 4 and 5 represent results obtained at the SH SAW wavelength of 60 μm. A similar behavior was observed at the 50 μm wavelength.

4. Conclusion

In conclusion, we have observed peculiarities of the light diffraction by SH SAWs in 36° rotated YX $LiTaO_3$ that cannot be explained by the simple model on the basis of Fig. 3. According to [8–10], the surface skimming bulk wave (SSBW) is the dominant propagation mode on the free surface of 36° rotated YX $LiTaO_3$, whereas the leaky surface acoustic wave (LSAW) prevails on the metallized surface. We attribute the observed differences in maximum-diffraction incidence angle values to the conversion processes between the LSAW and SSBW induced by the metal film strip. However, the relationship between SSBWs and LSAWs on 36° rotated YX $LiTaO_3$ has not been sufficiently elucidated. The velocities of both waves are very similar making their separation difficult. Further studies of acousto-optic effects involving both of these waves are required.

Acknowledgments

The work at Vilnius University was supported by the Research Council of Lithuania under Project No. MIP-057/2014. The work at RPI was supported by the US Army Research Office under Cooperative Research Agreement (Program Manager Dr. Meredith Reed).

References

[1] K.Y. Hashimoto, *Surface Acoustic Wave Devices for Telecommunications: Modelling and Simulation*, Springer, Berlin 2000.

[2] K. Nakamura, M. Kazumi, H. Shimizu, in: *Ultrason. Symp. Proc. 1977*, Eds. J. deKlerk, B.R. McAvoy, IEEE, Phoenix 1977, p. 819.

[3] C.K. Campbell, *Surface Acoustic Wave Devices for Mobile and Wireless Communications*, Academic Press, San Diego 1998.

[4] J. Kondoh, *Electron. Commun. Japan* **96**, 41 (2013).

[5] A. Holm, Q. Sturzer, Y. Xu, R. Weigel, *Microelectron. Eng.* **31**, 123 (1996).

[6] D. Čiplys, R. Rimeika, in: *Proc. 20th Int. Congress on Sound and Vibration (ICSV20)*, Eds. M.J. Crocker, M. Pawelczyk, B. Paosawatyanyong, IIAV, Bangkok 2013, CD-ROM.

[7] A. Yariv, P. Yeh, *Optical Waves in Crystals*, Wiley, New York 1984.

[8] K.Y. Hashimoto, M. Yamaguchi, H. Kogo, in: *Ultrasonics Symp. Proc. 1983*, Ed. B.R. McAvoy, IEEE, Atlanta 1983, p. 345.

[9] K. Yamanouchi, M. Takeuchi, in: *Proc. 1990 Ultrasonics Symp.*, IEEE, Honolulu 1990, p. 11.

[10] M. Yamaguchi, *Jpn. J. Appl. Phys.* **42**, 2909 (2003).